Cellulose (2019) 26:9071–9083
https://doi.org/10.1007/s10570-019-02696-3

ORIGINAL RESEARCH

Cellulose/biochar aerogels with excellent mechanical and thermal insulation properties

Lídia K. Lazzari · Daniele Perondi · Vitória B. Zampieri · Ademir J. Zattera · Ruth M. C. Santana

Received: 22 July 2019 / Accepted: 19 August 2019 / Published online: 28 August 2019

Abstract Aiming at investigating the use of alternative materials for the production of thermal insulation and, mainly, to replace the carbon structures (graphene and nanotubes), extensively used in the development of aerogels, the present study had the objective to produce cellulose/biochar aerogels and to evaluate their properties. The aerogels were produced from *Pinus elliottii* cellulose fibers and biochar produced from these fibers. The materials were characterized in their physical, thermal and mechanical properties. They were extremely light and porous, with a density between 0.01 and 0.027 g cm^{-3} and porosity between 93 and 97%. Several percentages of biochars were added to the cellulose suspension (0–100% w/w). The use of 40 wt% biochar provided a 60% increase in the compressive strength of the aerogel in relation to the cellulose aerogel. Besides that, the addition of this carbonaceous structure did not influence significantly the thermal conductivity of the aerogels, which presented a thermal conductivity of 0.021–0.026 W m^{-1} K^{-1}. The materials produced in the present research present a great potential to be used as insulators due to the low thermal conductivity found, which was very similar to the thermal conductivity of the air and also of commercial materials such as polyurethane foam and expanded polystyrene.

Keywords *Pinus elliottii* cellulose · Biochar · Carbon structure · Aerogel · Thermal insulation

Introduction

According to data from the International Energy Agency (IEA 2019), in the member countries in 2016, the residential sector accounted for 20% of energy consumption. In Brazil, in 2017 alone, the sector accounted for 28.8% of energy consumption (EPE 2018). Given that this percentage is a considerable part of the total energy consumption in the sector, there is a need to improve the energy performance of buildings by reducing the energy consumed. Considering that the orientation of a building and its architectural features are subject to constraints imposed by the densely built urban environment and also by architectural desires and restrictions, thermal

Electronic supplementary material The online version of this article (https://doi.org/10.1007/s10570-019-02696-3) contains supplementary material, which is available to authorized users.

L. K. Lazzari (✉) · R. M. C. Santana
Post Graduation Program in Mining, Metallurgy and Materials Engineering, Universidade Federal do Rio Grande do Sul, Porto Alegre, RS, Brazil
e-mail: lidia_lazzari@yahoo.com.br

D. Perondi · V. B. Zampieri · A. J. Zattera
Post-Graduation Program in Process and Technology Engineering, Universidade de Caxias do Sul, Francisco Getúlio Vargas Street, 1130, Bloco V - Room 408B, Bairro Petrópolis, Caxias do Sul, RS, Brazil

insulation remains a vital tool for optimizing the energy behavior of buildings (Papadopoulos and Giama 2007).

Materials, or fluids, of low thermal conductivity are considered thermally insulating, that is, they offer resistance to heat transfer between the system and the medium. In civil construction, they are used to prevent internal heat from spreading to the external environment. In this way, synthetic materials such as polyurethane (PU) and expanded polystyrene (EPS) are used on a large scale. The insulation capacity of a material is measured according to the thermal conductivity, that is, the lower the thermal conductivity, the greater the insulation capacity (Silva 2013).

In order to minimize the energy consumption of a building, by means of thermal protection, conductivity values of insulation materials (values less than 0.04 W m^{-1} K^{-1}) are in constant development. Among the most used categories of insulation materials are inorganic fibers (glass wool and rock wool) and organic foams (expanded polystyrene and polyurethane foams). These materials have a high performance in heat transfer resistance. However, their use causes some adversities such as: emission of greenhouse gases during their production, release of toxic gases when vaporized and high flammability (Cetiner and Shea 2018; Papadopoulos and Giama 2007; Silva 2013). Thus, the research and development of more sustainable and minimally processed insulators, such as aerogels, become fundamental.

Aerogels (porous solids) are considered very interesting materials for thermal insulation purposes because they present a high performance as a result of their extremely low thermal conductivity. In addition, they are characterized by their highly porous structure, reduced solids content and highly specific surface area. These properties make aerogels suitable for thermal insulation applications, electrodes in supercapacitors, advanced catalyst carriers and adsorbents (Du et al. 2013; Lei et al. 2018).

In recent years, the development of aerogels produced from different allotropic forms of carbon, such as graphene and nanotubes, attracted attention because of their superior properties, such as electrical and thermal conductivity, low density and mechanical strength. However, the high cost and toxicity of precursors added to the difficult and expensive technologies they require, as well as the equipment involved in the preparation, hinder their large-scale production (Hu et al. 2014; Lei et al. 2018).

Several authors present research on the development of cellulose aerogels and allotropic carbon forms, such as graphene oxide (Ge et al. 2018; Mi et al. 2018; Wan and Li 2016) and carbon nanotubes (Cong et al. 2018; Hwang et al. 2018) (as carbon source) for different applications, including thermal insulation. The results found in these studies show that the addition of these carbon structures to the cellulose aerogels does not present changes in the thermal conductivity of the same. The thermal conductivity of the cellulose aerogels (CMC)/graphene oxide (GO) remained around 0.04 W m^{-1} K^{-1} with the addition of 5% GO to the mass of CMC used (Ge et al. 2018). And for polyglycolic alcohol (PVA) aerogels, cellulose nanofibers (CNFs) and graphene oxide nanoparticles (GONSs) the thermal conductivity was 0.045 W m^{-1} K^{-1}.

Furthermore, according to the studies carried out by the aforementioned authors, the addition of carbon structures in cellulose aerogels improves the mechanical properties of the material, where the compression modulus and the resistance are larger proportionally with the increase of the carbonaceous particles content, which can be attributed to the well-defined crystalline structure of these materials (Ge et al. 2018; Zheng et al. 2013).

With an environment of harnessing industrial and agricultural waste for the production of new thermal insulators has also been much studied. The use of organic precursors subjected to the pyrolysis process, which thermally decomposes the biomass structure, produces carbonaceous solid waste (biochar) and condensable and non-condensable vapors. This biochar is highly carbonous and therefore has a high energy value. In addition, it is an added-value product that can be used for many purposes (Basu 2010; Lee et al. 2013; Skouteris et al. 2015). Cellulose is not only a qualified raw material for the preparation of carbon materials and is attractive due to its low cost, viability, abundance and non-toxicity, but also a renewable resource (Bakierska et al. 2014; Chang et al. 2010; Dunnigan et al. 2018; Han et al. 2016; Lazzari et al. 2018).

Cellulose aerogels, being produced from renewable sources (plants, wood, algae and animals), can be considered environmentally friendly and can reduce the manufacturing cost due to the low cost of the raw

material. The low density of cellulose fibers provides cellulose aerogels with high porosity and high surface area, as well as high mechanical strength due to the three-dimensional structure formed by cellulose fibers (Feng et al. 2015; Xiao et al. 2015; Innerlohinger et al. 2006).

Within this context, cellulose/biochar aerogels were produced aiming at their use thermal insulators. *Pinus elliottii* pulp was used as raw material for the production of aerogel and also for biochar, making it possible to add a high value to this biomass allied to a low processing cost. The thermal, chemical and morphological properties of the aerogels were studied in order to evaluate their use as thermal insulators.

Materials and methods

Materials

The cellulose used in the present work was supplied by the company Trombini (Brazil). The type of cellulose used was the unbleached long fiber of *Pinus elliottii*. Cellulose was further characterized as to its composition, chemical, physical, thermal and morphological properties.

Obtaining the *Pinus elliottii* cellulose biochar

Initially the cellulose was comminuted in a knife mill (10 mm size) and dried in an oven at 105 °C for 24 h, so that pyrolysis could be performed in a bench reactor, which operates in a batch system. A detailed description of this equipment was recently reported by Perondi et al. (2017). The parameters used in the pyrolysis were: heating rate of 5 °C min^{-1}, final operating temperature of 800 °C and N_2 flow of 150 mL min^{-1}. The cellulose mass used in the feed was approximately 35 g. The biochar was obtained after the cooling stage of the reactor. Due to differences in the size of the resulting particles, maceration was conducted, resulting in homogenous particles.

Obtaining the cellulose/biochar aerogels

The cellulose/biochar aerogels were produced according to the methodology presented by Lazzari et al. (2017). Initially, *Pinus elliottii* cellulose was milled in a knife mill. Thereafter, a suspension was produced with distilled water and cellulose in the concentration of 1.5% (w/w). This suspension was later placed in a Masuko Sangyo stone micronizer, model MKCA6-2J (Japan) for the fiber milling for 5 h (Neves et al. 2019). The aerogels were produced from the actual cellulose concentration (1.43 and 0.715% w/w) and biochar (0.5, 10, 20, 40, 80 and 100% w/w, relative to the cellulose mass). In the following step, the cellulose suspension was centrifuged for 5 min at 4500 rpm. To the supernatant, a certain concentration of biochar was added and maintained on mechanical agitation for 5 min for homogenization of the mixture. Thereafter, the supernatant was mixed to the pellet, also by mechanical agitation and for 5 min. The suspension obtained after the milling process was sonicated for 30 min in a Sonics Sonifier Model VC505 Sonifier, with an amplitude of 50% measured in relation to the maximum equipment capacity (500 W). Then, metal molds were used to condition the samples. These molds have the following dimensions: 5 cm (side) × 2.5 cm (thickness). The samples (packaged in the molds) were then frozen in a Panasonic MDF PRO Series freezer at a temperature of − 80 °C for 24 h. Freeze drying was carried out in a Lio Top lyophilizer, Model L101 (Brazil). The samples were placed in a chamber and subjected to vacuum at a temperature of − 40 °C for about 70 h for the sublimation of the ice and drying of the aerogel.

Characterization of the aerogels

The bulk density of the aerogels was measured according to ASTM D1622-08, and calculated according to Eq. 1.

$$\rho_{aerogel} = \frac{m}{v} \quad (1)$$

in which $\rho_{aerogel}$ is the apparent density of aerogel (g cm^{-3}); m is the mass of the aerogel (g) and v is the volume of the aerogel (cm^3).

The porosity of the aerogels was determined by a method presented by Sehaqui et al. (2011), by using Eq. 2.

$$\text{Porosity}\,(\%) = \left(1 - \frac{\rho_{aerogel}}{\rho_{cellulose}}\right) \times 100 \quad (2)$$

in which $\rho_{aerogel}$ is the apparent density of aerogel (g cm^{-3}) and $\rho_{cellulose}$ is the apparent density of cellulose (0.39 g cm^{-3}).

The thermal properties of the aerogels were evaluated by thermogravimetry (TG) using a Shimadzu model, TGA-50, with a heating rate of 10 °C min^{-1}, from 30 to 800 °C, under a nitrogen atmosphere (N_2) with a flux of 50 mL min^{-1}.

Thermal conductivity of aerogels

The thermal conductivity of the aerogels was determined according to the norm NBR 15220-5 (2003). Samples with the following dimensions were used: 50 × 50 × 20 mm width, length and thickness, respectively, in duplicate. The heat flux applied to the system was determined by measurements with PSI-20 glass wool (density 0.020 g cm^{-3}), which is known for its thermal conductivity (0.038 W m^{-1} K^{-1}). The glass wool was supplied by Tecnotermo Isolantes Térmicos (Brazil). The thermal conductivity of the samples was determined by Eq. 3.

$$\lambda = \frac{q \times e}{\Delta t} \tag{3}$$

in which λ is the thermal conductivity (W m^{-1} K^{-1}); q is the heat flux density (W m^{-2}); *e* is the thickness of the sample (m) and Δt is the temperature difference between the hot and the cold faces of the sample (K).

Compressive strength of aerogels

The compressive strength tests were performed in a universal testing machine (EMIC, model DL 2000, Brazil), with a compression speed of 1.3 mm min^{-1}. The assay was performed in duplicate, the samples were 5 cm (side) × 2.5 cm (thickness). They were used to measure the tension required to reduce the thickness of the specimen in 20, 50 and 70% of their initial thickness, and were adapted from ASTM D695-15.

Results and discussion

Cellulose aerogels

The cellulose suspension was produced from a mixture with 1.5% (w/w) cellulose. However, the actual concentration of cellulose after the milling process was 1.43 ± 0.02%. This decrease occurred due to the losses in the walls of the mill. Therefore, the cellulose concentration of the AC-1 and AC-2 aerogels was 1.43 ± 0.02% and 0.715 ± 0.02%, respectively (as reported in Table 1).

Table 1 presents the results of apparent density and calculated porosity of AC-1 and AC-2 aerogels. Density values between 0.010 and 0.019 g cm^{-3} and porosity between 97.3 and 95.1% were results found for samples AC-1 and AC-2, respectively. It is possible to verify that the apparent density is proportional to the cellulose concentration used, since the AC-1 aerogel had an apparent density about 50% higher than the aerogels AC-2.

The porosity is inversely proportional to the apparent density, that is, the greater the apparent density of the aerogel, the smaller its porosity. The aerogel that presented greater porosity was AC-2, at about 97%. This result, is due to the lower concentration of fibers present in it.

The process of mechanical grinding of cellulose promotes defibrillation and breaking of fibers from the micrometric scale to the nanometric. Besides, it more economical and beneficial to the environment as no chemical reagents are used. Figure 1 shows the micrographs of cellulose and cellulose/biochar aerogels.

In the observed structure of the cellulose aerogels in Fig. 1b, d, it is possible to notice that the fibers remain long, with length in the micrometric and agglomerated. On the other hand, the thickness of the fibers decreased, presenting several fibers with thickness in nanoscale. In addition, due to the hydrophilic nature of the cellulose, the fibers agglomerate when in suspension. Thus, even after drying the aerogels, there is the formation of extended "sheets" forming macroscopic open channels and large pores with several micrometers wide, which connect the different cells and thin sheets of aerogel (Aulin et al. 2010).

Rapid freezing is known to be accompanied by the formation of amorphous ice which, in turn, can lead to a more homogeneous fibrillar aerogel structure with smaller pores and less pronounced structure. In contrast, slow freezing increases the formation of non-amorphous ice (crystals) which contributes to the formation of "sheets". The structure of aerogel is therefore directly related to the size and distribution of ice crystals in the frozen system. In addition, the thickness of the aerogels plays an important role in the

Table 1 Nomenclature, composition, density and porosity of cellulose/biochar aerogels

Nomenclature	Cellulose concentration (% w/w)	Biochar concentration[a] (% w/w)	Apparent density (g cm^{-3})	Porosity (%)
AC-1	1.43 ± 0.02	0.0	0.019 ± 0.0005	95.15 ± 0.12
AC-1.B5	1.43 ± 0.02	5.0	0.021 ± 0.0005	94.55 ± 0.12
AC-1.B10	1.43 ± 0.02	10.0	0.025 ± 0.001	93.67 ± 0.21
AC-1.B20	1.43 ± 0.02	20.0	0.024 ± 0.001	93.93 ± 0.13
AC-1.B40	1.43 ± 0.02	40.0	0.022 ± 0.001	94.31 ± 0.15
AC-1.B80	1.43 ± 0.02	80.0	0.026 ± 0.001	93.31 ± 0.20
AC-1.B100	1.43 ± 0.02	100.0	0.027 ± 0.001	93.10 ± 0.17
AC-2	0.715 ± 0.02	0.0	0.010 ± 0.0002	97.35 ± 0.06

[a]The biochar concentration was a function of the cellulose concentration

freezing rate. Therefore, thicker samples freeze more slowly (Aulin et al. 2010).

Figure 2a shows the thermogravimetry of the *Pinus elliottii* cellulose sample and the AC-1 and AC-2 aerogels. The cellulose aerogels showed a mass loss below 100 °C, due to the presence of moisture in the samples. In addition, the highest percentage of mass loss was observed between 250 and 450 °C, due to the degradation of the hemicelluloses, cellulose and a lower degradation of part of the lignin.

A difference is noted in T_{onset} (temperature at which sample degradation starts) and T_{max} (temperature at which the rate of degradation is maximal), as shown in Table 2. These temperatures of the cellulose aerogels decreased in relation to the *Pinus elliottii* cellulose fiber, probably due to the increase of the specific surface area obtained after the mechanical process, which facilitates the degradation process when compared to the original material, and contributes to thermal stability decrease (Zanini et al. 2017). The residual mass of the aerogels had a slight decrease compared to the original cellulose.

Gupta et al. (2018) obtained an increase in the thermal stability of the aerogels due to the presence of fibers on the nanometer scale in their cellulose aerogels. However, they performed a chemical treatment before the mechanical milling on the fibers for the removal of lignin, hemicellulose and pectin. This treatment increased the initial degradation temperature to about 80 °C.

Figure 3a shows the stress × strain curves and the compressive strength of aerogels AC-1, AC-1.B40 and AC-2.

The stress × strain curves presented in Fig. 3a present different stages according to the slope of the curve: a linear stage with a fixed slope of the curve, a long regime of elastic–plastic deformation, and a stage in which the compression stress increases significantly due to the gradual densification of the porous structure. This behavior was also observed for silica aerogels reinforced with glass fibers (Li et al. 2017) and cellulose nanofibers aerogels (Jiménez-Saelices et al. 2017).

The AC-1 aerogel has a compressive strength about 35% higher than the AC-2 aerogel, for deformation of 70%. According to Jiménez-Saelices et al. (2017) the apparent density (from 0.010 to 0.019 g cm^{-3} of aerogels AC-2 and AC-1, respectively) causes an increase in pore wall thickness, causing a greater resistance of the structure to curvature and collapse of the wall cells.

The statistical analysis was performed for the deformation of 70% of the specimen, as shown in Table S.2 (complementary information). Between AC-1 and AC-2 (identified by 2 different letters in Fig. 3b) there is a significant difference in compressive strength. Therefore, the cellulose concentration impacts significantly, that is, the amount of cellulose used influences the compressive strength of the cellulose aerogels for a 70% deformation of the sample.

Figure 4 shows the thermal conductivity of the cellulose/biochar aerogels. The AC-1 and AC-2 cellulose aerogels presented thermal conductivity of 0.024 and 0.021 W m^{-1} K^{-1}, respectively.

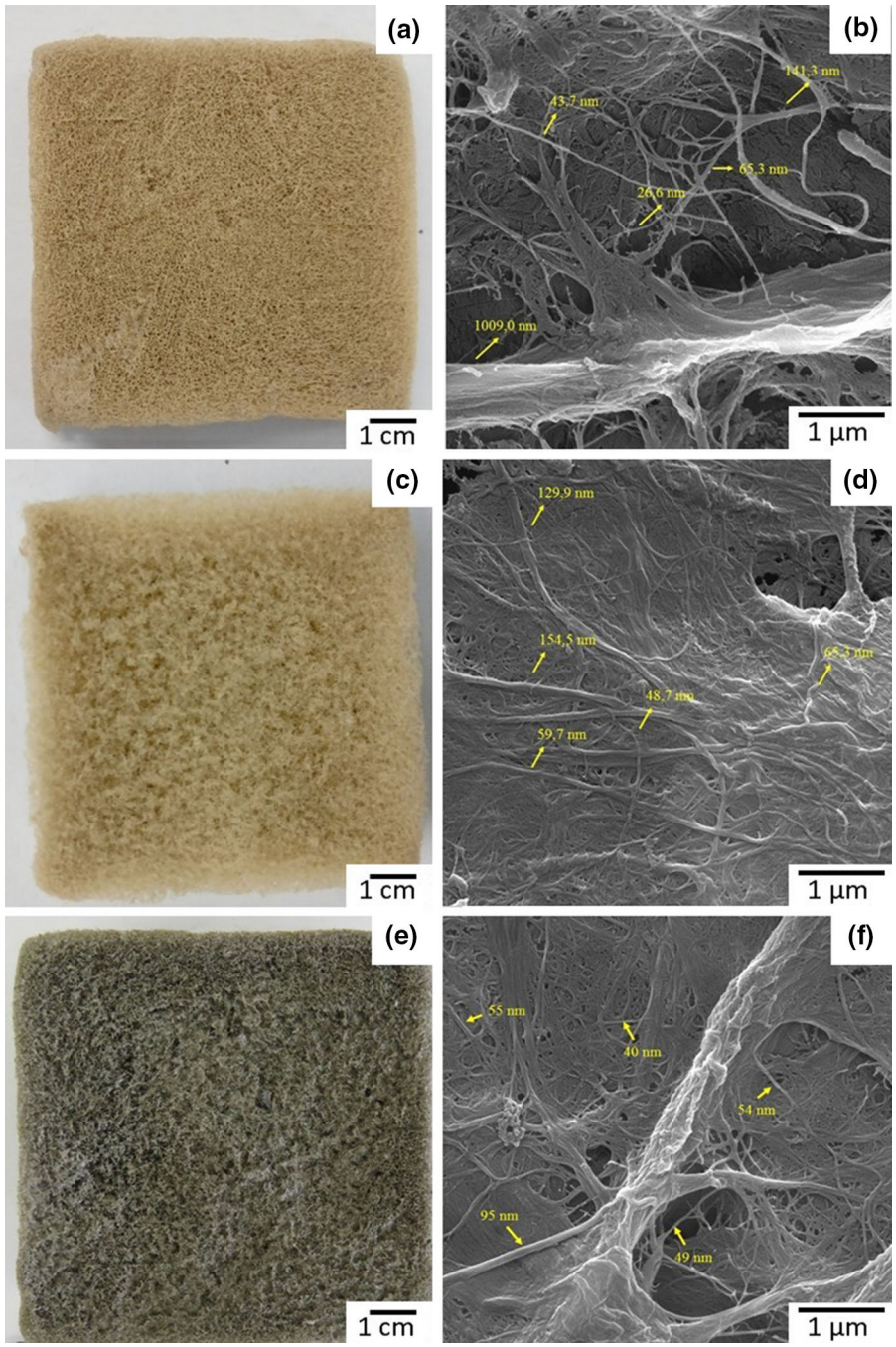

Fig. 1 Photos of aerogels: AC-1 (**a**); AC-2 (**c**) and AC-1.B40 (**e**). Micrographs of aerogels: AC-1 (**b**), AC-2 (**d**) and AC-1.B40 (**f**)

According to the statistical analysis presented in item S.5 (complementary information) and multiple comparison of means (Table S.3), we concluded that the concentration of cellulose does not cause significant difference, i.e. the amount of cellulose used does not influence the conductivity of the aerogels. This is because, as can be seen from Table 1, there is not a considerable difference in the porosity of aerogel, about 2% only.

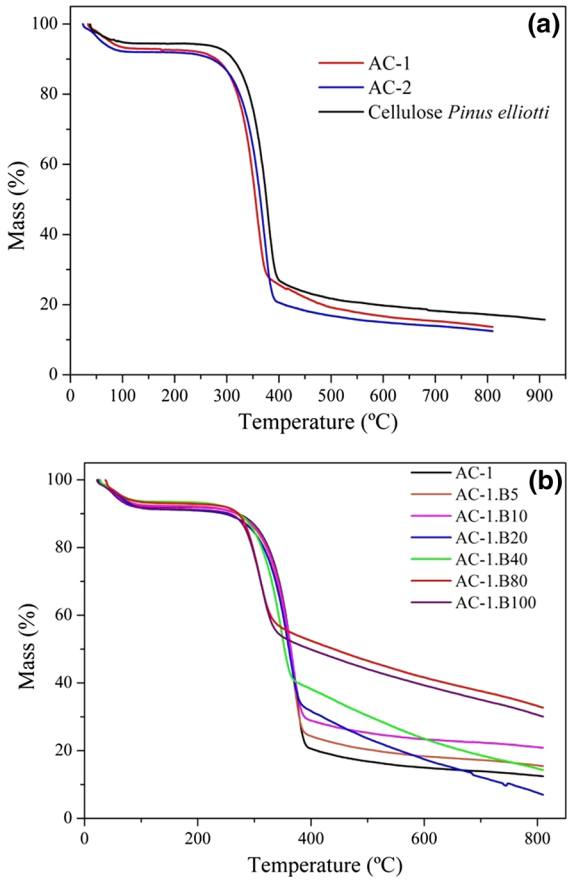

Fig. 2 Thermogravimetry of *Pinus elliottii* fiber and aerogels of **a** cellulose and **b** cellulose/biochar

The high porosity of the aerogels (more than 95% of the aerogel structure is composed by air) provides them with a thermal conductivity inferior to the thermal conductivity of the air (0.026 W m^{-1} K^{-1}) (Incropera et al. 2007).

Karadagli et al. (2015) used cellulose fibers to produce aerogels by extrusion. The authors evaluated the influence of fiber concentration (0.5–6 % w/w) on bulk density (0.009 and 0.137 g cm^{-3}), porosity (99 and 91%), compressive strength ($\sim$ 0.3 to 1.5 MPa, for deformation of 50% of the specimen) and thermal conductivity (0.04 and 0.075 W m^{-1} K^{-1}). The results found by the authors showed the same behavior found in the present study for density and porosity. However, for the thermal conductivity, the authors found values superior to those found in the present study, which shows that AC-1 and AC-2 present a better thermal insulation than others aerogels. Regarding the compressive strength, the authors found extremely high values when compared with the aerogels of the present study.

By means of statistical analysis, we found that the cellulose concentration significantly influenced the compressive strength of the aerogels, because there is an increase in the fraction of solids present in AC-1 aerogel compared to AC-2 aerogel. On the other hand, in the thermal conductivity test, the cellulose concentration did not present significant influence. Considering these tests as the main results for the determination of the cellulose concentration for the production of the aerogels, it was decided to choose sample AC-1, with cellulose concentration of 1.43% for the continuation of this research, mainly due to its compressive strength being superior to the sample AC-2, since the thermal conductivity is not influenced by cellulose concentration.

Cellulose/biochar aerogels

Figure 5 shows the cellulose/biochar aerogels produced with different concentrations of biochar,

Table 2 Results of the analysis of thermogravimetry of the *Pinus elliottii* cellulose fiber, cellulose aerogels and cellulose/biochar aerogels

Sample	T_{onset} (°C)	$T_{máx}$ (°C)	Residual mass (%)
Pinus elliottii cellulose	342	382	15.80
AC-1	333	372	12.50
AC-1.B5	316	370	15.80
AC-1.B10	323	368	20.98
AC-1.B20	315	360	5.14
AC-1.B40	297	349	14.38
AC-1.B80	276	313	32.83
AC-1.B100	272	315	30.08
AC-2	315	358	13.70

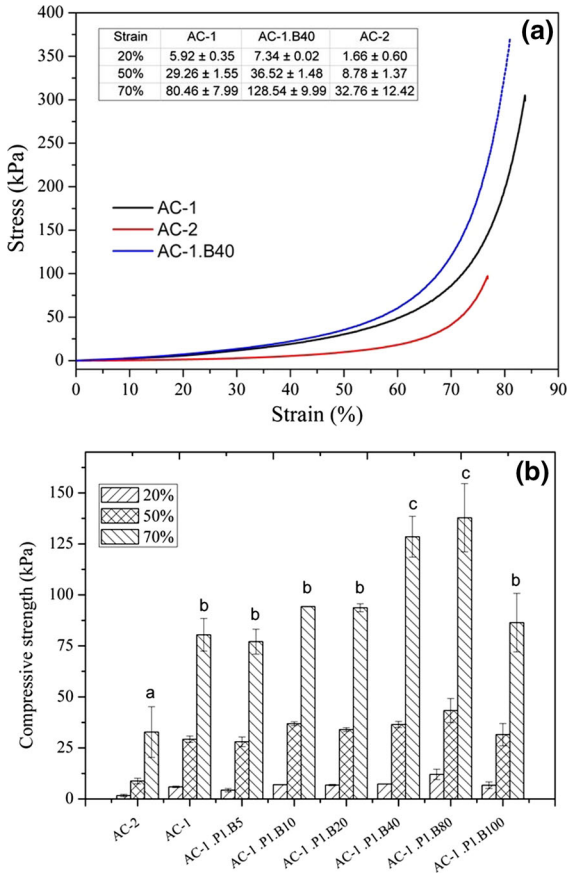

Fig. 3 **a** Stress × strain curves and **b** Compressive strength of *Pinus elliottii* AC-1 and AC-2 cellulose aerogels with deformation of 20, 50 and 70% of the specimen. *Note*: Different letters indicate the significant difference between groups

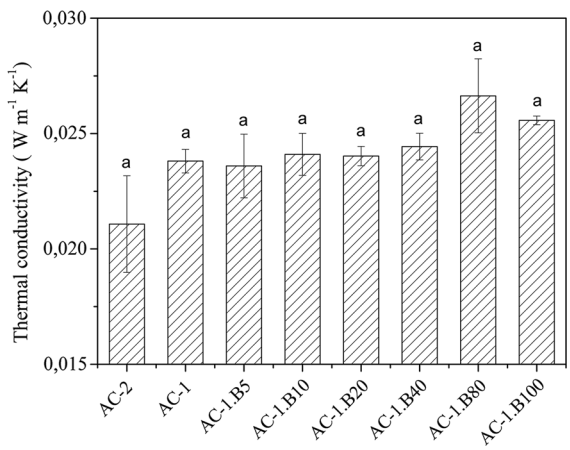

Fig. 4 Thermal conductivity of cellulose and cellulose/biochar aerogels

according to the nomenclature presented in Table 1. Due to the increase of the concentration of biochar in the cellulose aerogel, its coloration changes gradually into a dark gray tone. The aerogels have a uniform coloration, showing that the mixture of the biochar in the cellulose suspension was homogeneous. In addition, the three-dimensional structure of aerogels is composed of pores of different sizes. However, by adding the biochar, the pore size reduces, due to the higher amount of solids in the cellulose/biochar suspension.

Table 1 shows the bulk density and porosity of the cellulose/biochar aerogels. With the addition of the biochar to the cellulose suspension, the calculated value of the apparent density of the aerogels presents a slight increase, from 0.0189 to 0.0269 (higher value found for aerogel AC-1.B100). As the porosity is inversely proportional to the bulk density, the porosity decreased from 95.15 to 93.10% for aerogels AC-1 and AC-1.B100, respectively.

Yang et al. (2016) also observed this behavior in their aerogels of microcrystalline cellulose and graphene nanoplatelets, having a two fold increase in density for aerogel with cellulose/nanoplatelet concentration of 1:1 compared to microcrystalline cellulose aerogel. Consequently, there was a decrease in porosity of about 5% between these same aerogels.

Figure 1e, f present the image and micrograph, respectively, of aerogel AC-1.B40, in order to compare the micrographs of this aerogel with AC-1 and AC-2 aerogels. The structure of the aerogel was not altered with the addition of the biochar, remaining with long and very agglomerated fibers. The fact that biochar is produced from cellulose itself hinders its identification, and through them it can be noticed that there was homogenization of the biochar to the cellulose suspension.

Several authors report that the addition of graphene oxide (GO), a carbonaceous structure such as biochar, in cellulose aerogels provides changes in the structure of aerogels, for example, the porous structure becomes more heterogeneous, the interaction and entanglement of the GO and cellulose form denser networks, the porous structure of the wall is replaced by a lamellar structure, among others (Ren et al. 2018; Wan and Li 2016; Xiang et al. 2019).

Figure 2b shows the thermogravimetry of the cellulose/biochar aerogels, where it can be observed that the addition of the biochar, even in homogeneity

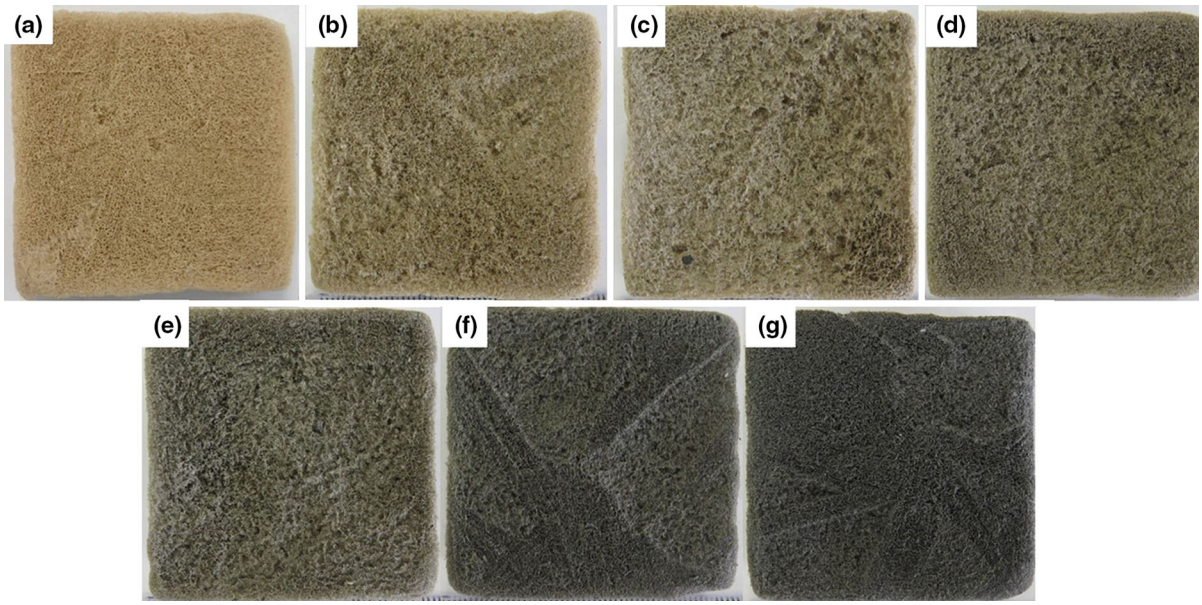

Fig. 5 Cellulose/biochar aerogels: **a** AC-1, **b** AC-1. B5, **c** AC-1.B10, **d** AC-1.B20, **e** AC-1.B40, **f** AC-1.B80 and **g** AC-1.B100

with the cellulose suspension and having already had its organic matter degraded, decreased the thermal stability of the aerogels.

The presence of the biochar in the aerogels causes the decrease of the T_{onset} and T_{max} temperatures (obtained by thermogravimetry derived from the curves), as can be seen in Table 2. However, its presence increases the residual mass, due to the submission of the raw material to the pyrolysis process, before the production of the aerogel, during which the organic matter was degraded.

In a study carried out by Wan and Li (2016) the authors also noted this behavior among their samples, where T_{onset} decreased from 363 to 353 °C in the aerogels of bamboo fiber cellulose and the aerogel with 5% of graphene oxide (GO), respectively. Furthermore, the authors reported that there is no mass loss related to the decomposition of the oxygen receptor groups on the surface of the GO due to deoxygenation and low proportion of the same in the aerogels.

Figure 3a shows the stress–strain curves of aerogels AC-1 and AC-1.B40. Curves exhibit foam-like deformation behavior. The aerogels suffered a plastic deformation, a deformation of 0–70%, irreversibly. After this region, due to the densely compressed structure, the aerogels become resistant, and therefore the tension increases rapidly. Ge et al. (2018) observed the same behavior for their GO/CMC aerogels, but in the deformation range of 0–7%, there was an elastic deformation. The authors obtained a 62% increase in compressive strength with the addition of 5% graphene oxide in CMC aerogels.

Figure 3b shows the compressive strength of the cellulose/biochar aerogels for deformations of 20, 50 and 70% of the sample. In all evaluated deformation, the behavior is the same, presenting a slight tendency to increase until the concentration of 80% of biochar in cellulose mass and, subsequently, a considerable decrease of resistance takes place, of about 60%. For deformation of 70% of the specimen, there was an increase from 80 to 128 kPa (aerogels AC-1 and AC-1.B40, respectively), about 60% greater.

Due to the high standard deviation associated with some aerogels, a statistical analysis was presented in Table S.2 (complementary information) and multiple comparison of means presented in Table S.3 (complementary information). From the results, we concluded that the compressive strength of the cellulose/biochar aerogels presents a significant difference, that is, the amount of biochar used influences the compressive strength between some cellulose1/biochar aerogels for deformation of 50% of the sample (see association of letters).

Considering that the aerogels AC-1.B40 and AC-1.B80 had the highest resistance values (128 and

137 kPa, respectively), and that between the two there is no significant difference (both are identified with the letter "*c*"), it can be considered that with the addition of 40% of biochar in relation to the mass of cellulose one obtains the greatest resistance to the compression of the aerogels.

Mi et al. (2018) obtained the greatest compressive strength in their study with the increase of graphene oxide in the aerogels of cellulose nanofibers, and attributed this improvement to the stiffness of the graphene sheets. Ge et al. (2018) compared the compressive strength of aerogels of carboxymethyl cellulose and cellulose/graphene oxide nanosheets (GOS), and with the addition of 5.0% of GOS, the compressive strength reached 349 kPa, which were 1.6 times that of CMC aerogels. This increase is attributed to the good dispersion of GOS in the cellulose suspension and the strong interfacial adhesion to the matrix.

Figure 6 shows the aerogels AC-1 and AC-1.B40 during the compression test. It is possible to verify that the aerogel has a rigid structure, because after the aerogel load is removed, it does not return to its original state, having a plastic deformation known as permanent deformation. At the end of the trial, the aerogels were reduced by about 80% of their original height.

Figure 4 shows the thermal conductivity of the cellulose/biochar aerogels. The values found ranged from 0.024 to 0.027 W m^{-1} K^{-1}, the first being found for AC-1 and the second for AC-1.B80. Due to the small difference found, a statistical analysis of the results was performed, as presented in Table S.5 (complementary information). The conductivity of the aerogels did not present significant difference, that is, the addition of the biochar did not influence in the thermal conductivity of the aerogels.

Considering that the thermal conductivity of aerogels is determined mainly by the thermal conductivity factor of the solid material, density and pore size, and since having a significant, yet very small, difference in density and porosity of the aerogels, the absence of significant differences in the thermal conductivity of non-aerogels is justified (Wiener et al. 2006).

According to Wiener et al. (2006), the transport of heat through a porous solid, consists of radioactive, gaseous and solid contributions. Therefore, the change in thermal conductivity is due to changes in the solid phase of the material. In the aerogels produced in the present study, there were no changes in structure due to the addition of the biochar, as shown in Fig. 1. The influence that the biochars caused in the aerogels was the increase of the apparent density and the decrease of the porosity, which resulted in an increase in

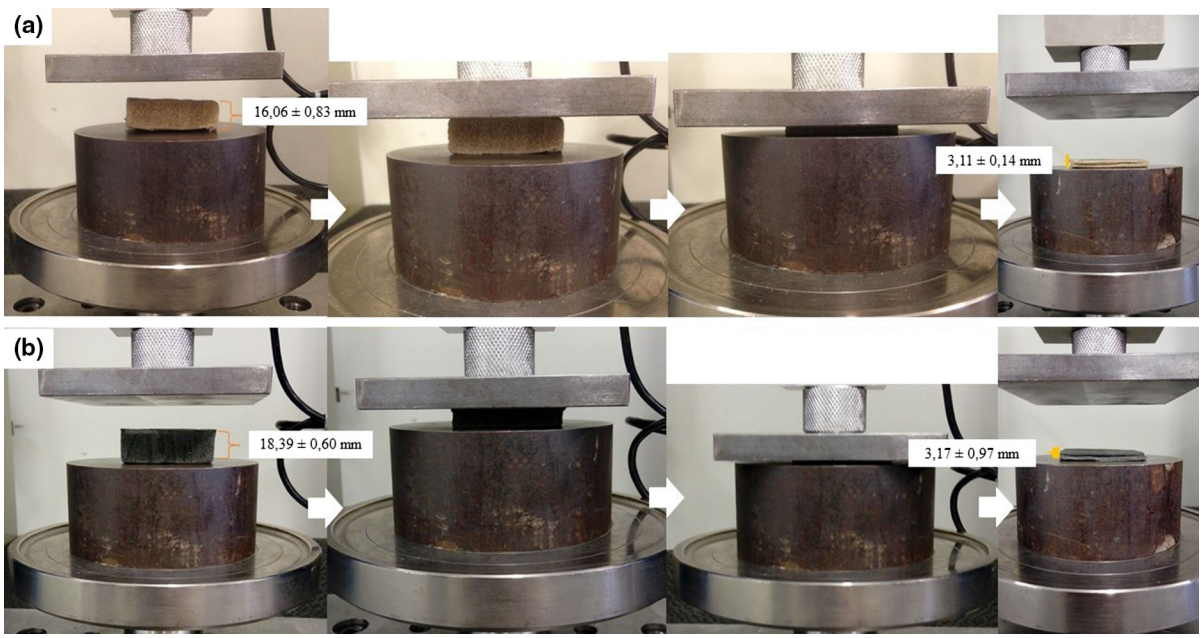

Fig. 6 Images of the compression test of cellulose/biochar aerogels. **a** AC-1 and **b** AC-1.P1.B40

Table 3 Thermal conductivity of thermal insulators materials

Sample	Thermal conductivity (W m^{-1} K^{-1})	Reference
AC-1.B40	0.024	–
Polyurethane foam	0.02–0.03	Zhang et al. (2017)
CMC/GO aerogels	0.04	Ge et al. (2018)
Silica aerogel	0.0338	Zhao et al. (2018)
Recycled cellulose aerogel	0.032	Nguyen et al. (2014)
Expanded polystyrene	0.04	Silva (2013)
Cellulose nanofiber aerogel	0.018–0.028	Jiménez-Saelices et al. (2017)
Silica cellulose aerogel	0.0236	Fu et al. (2016)
Wood waste	0.048–0.055	Cetiner and Shea (2018)

conductivity, but not enough to show significant differences between them.

Ge et al. (2018) developed aerogels of carboxymethylcellulose (CMC) and graphene oxide (GO) in a concentration of up to 5% mass of cellulose. When comparing cellulose aerogel with CMC/GO aerogels, both the thermal conductivity factor (between 0.038 and 0.042 W m^{-1} K^{-1}) and the density (between 24.3 and 25.5 kg m^{-3}) of the composite aerogel increased at a small rate after the addition of GO, so the solid-state thermal conductivity increased as well. Furthermore, in the absence of obvious changes in density and pore structure, the thermal conductivities of aerogels tended to increase slowly with increasing GO content. This is because the thermal conductivity factor of the aerogel increased with increasing GO content.

The thermal conductivity of the aerogels found in the present study, about 0.025 W m^{-1} K^{-1}, is comparable to the thermal conductivity of commercial materials such as polyurethane foams and expanded polystyrene and other thermal insulator aerogels, as noted in Table 3.

Conclusion

In relation to the cellulose concentration, the results obtained in the statistical analysis present in Supplementary Material were evaluated, and, the thermal conductivity and compressive strength tests were considered the main results for the determination of the cellulose concentration for the production two aerogels. These results were the basis for the choice of the aerogels AC-1, with a cellulose concentration of 1.43% for the continuation of the studies in the present study, mainly due to its compressive strength being superior to AC-2, given that the thermal conductivity is not influenced by the cellulose concentration.

The cellulose/biochar aerogels produced presented good characteristics to be used as thermal insulators. Although they had a heterogeneous structure, the porosity was high, higher than 95%, and the bulk density (about 0.025 g cm^{-3}) was close to that of materials such as glass wool, widely used in construction. The addition of biochar did not increase the thermal stability of aerogels as expected. On the contrary, the higher the concentration used the lower the maximum degradation temperature. On the other hand, the biochar had no influence on the thermal conductivity of the aerogels (about 0.025 W m^{-1} K^{-1}), which was close to that of the polyurethane foams (0.02–0.03 W m^{-1} K^{-1}). However, an increase in the compressive strength of the cellulose/biochar aerogels (AC-1.B40) of 60% in relation to the cellulose aerogel (AC-1) can be verified.

For these, they presented more thermal insulation than aerogels produced with carbon structures as precursors, in addition to having very close compressive strength to these aerogels. Finally, the cellulose/biochar aerogels are promising for the thermal insulation application proposed for the present work.

Acknowledgments The authors are grateful for the National Council for Scientific and Technological Development (CNPq)

and the Foundation for Research Support of the State of Rio Grande do Sul (FAPERGS).

References

Aulin C, Netrval J, Wagberg L, Lindstrom T (2010) Aerogels from nanofibrillated cellulose with tunable oleophobicity. Soft Matter 6(14):3298–3305

Bakierska M, Molenda M, Majda D, Dziembaj R (2014) Functional starch based carbon aerogels for energy applications. Procedia Eng 98:14–19

Basu P (2010) Biomass gasification and pyrolysis: practical design and theory. Academic Press, Burlington

Cetiner I, Shea AD (2018) Wood waste as an alternative thermal insulation for buildings. Energy Build 168:374–384

Chang X, Chen D, Jiao X (2010) Starch-derived carbon aerogels with high-performance for sorption of cationic dyes. Polymer 51(16):3801–3807

Cong L, Li X, Ma L, Peng Z, Yang C, Han P, Wang G, Li H, Song W, Song G (2018) High-performance graphene oxide/carbon nanotubes aerogel-polystyrene composites: preparation and mechanical properties. Mater Lett 214:190–193

Du A, Zhou B, Zhang Z, Shen J (2013) A special material or a new state of matter: a review and reconsideration of the aerogel. Materials 6(3):941–968

Dunnigan L, Ashman PJ, Zhang X, Kwong CW (2018) Production of biochar from rice husk: particulate emissions from the combustion of raw pyrolysis volatiles. J Clean Prod 172:1639–1645

EPE (2018) Anuário estatístico de energia elétrica 2018. Empresa de pesquisa energética. http://www.epe.gov.br/en/publicacoes-dados-abertos/publicacoes/anuario-estatistico-de-energia-electrica. Accessed 25 Apr 2019

Feng J, Nguyen ST, Fan Z, Duong HM (2015) Advanced fabrication and oil absorption properties of super-hydrophobic recycled cellulose aerogels. Chem Eng J 270:168–175

Fu J, Wang S, He C, Lu Z, Huang J, Chen Z (2016) Facilitated fabrication of high strength silica aerogels using cellulose nanofibrils as scaffold. Carbohydr Polym 147:89–96

Ge X, Shan Y, Wu L, Um X, Peng H, Jiang Y (2018) High-strength and morphology-controlled aerogel based on carboxymethyl cellulose and graphene oxide. Carbohydr Polym 197(June):277–283

Gupta P, Singh B, Agrawal AK, Maji PK (2018) Low density and high strength nanofibrillated cellulose aerogel for thermal insulation application. Mater Des 158:224–236

Han S, Sun Q, Zheng H, Li J, Jin C (2016) Green and facile fabrication of carbon aerogels from cellulose-based waste newspaper for solving organic pollution. Carbohydr Polym 136:95–100

Hu H, Zhao Z, Wan W, Gogotsi Y, Qiu J (2014) Polymer/graphene hybrid aerogel with high compressibility, conductivity, and "sticky" superhydrophobicity. ACS Appl Mater Interfaces 6:3242–3249

Hwang HC, Woo JS, Park SY (2018) Flexible carbonized cellulose/single-walled carbon nanotube films with high conductivity. Carbohydr Polym 196:168–175

IEA (2019) Energy Efficiency Indicators Database. International Energy Agency. https://www.iea.org/statistics/efficiency/. Accessed 25 Apr 2019

Incropera FP, Dewitt DP, Bergman TL, Lavine AS (2007) Fundamentos de transferência de calor e massa. Wiley, New York

Innerlohinger J, Weber HK, Kraft G (2006) Aerocellulose: aerogels and aerogel-like materials made from cellulose. Macromol Symp 244:126–135

Jiménez-Saelices C, Seantier B, Cathala B, Grohens Y (2017) Spray freeze-dried nanofibrillated cellulose aerogels with thermal superinsulating properties. Carbohydr Polym 157:105–113

Karadagli I, Schulz B, Schestakow M, Milow B, Gries T, Ratke L (2015) The Journal of Supercritical Fluids Production of porous cellulose aerogel fibers by an extrusion process. J Supercrit Fluids 106:105–114

Lazzari LK, Zampieri VB, Zanini M, Zattera AJ, Baldasso C (2017) Sorption capacity of hydrophobic cellulose cryogels silanized by two different methods. Cellulose 24(8):3421–3431

Lazzari E, Schena T, Marcelo MCA, Primaz CT, Silva AN, Ferrao MF, Bjerk T, Caramao EB (2018) Classification of biomass through their pyrolytic bio-oil composition using FTIR and PCA analysis. Ind Crops Prod 111(November 2017):856–864

Lee Y, Park J, Ryu C, Gang KS, Yang W, Park YK, Jung J, Hyun S (2013) Comparison of biochar properties from biomass residues produced by slow pyrolysis at 500°C. Bioresour Technol 148:196–201

Lei E, Li W, Ma C, Liu S (2018) An ultra-lightweight recyclable carbon aerogel from bleached softwood kraft pulp for efficient oil and organic absorption. Mater Chem Phys 214:291–296. https://doi.org/10.1016/j.matchemphys.2018.04.075

Li C, Cheng X, Li Z, Pan Y, Huang Y, Gong L (2017) Mechanical, thermal and flammability properties of glass fiber film/silica aerogel composites. J Non-Cryst Solids 457:52–59

Mi HY, Jing X, Politowicz AL, Chen E, Huang HX, Turng LS (2018) Highly compressible ultra-light anisotropic cellulose/graphene aerogel fabricated by bidirectional freeze drying for selective oil absorption. Carbon 132:199–209

Nguyen ST, Feng J, Ng SK, Wong JPW, Tan VBC, Duong HM (2014) Advanced thermal insulation and absorption properties of recycled cellulose aerogels. Colloids Surf A 445:128–134

Neves RM, Lopes KS, Zimmermann MGV, Polleto M, Zattera AJ (2019) Cellulose nanowhiskers extracted from Tempo-oxidized curaua fibers. J Nat Fibers. https://doi.org/10.1080/15440478.2019.1568346

Papadopoulos AM, Giama E (2007) Environmental performance evaluation of thermal insulation materials and its impact on the building. Build Environ 42(5):2178–2187

Perondi D, Poletto P, Restelatto D, Manera C, Silva JC, Junges J, Collazo GC, Dettmer A, Godinho M, Vilela ACF (2017) Steam gasification of poultry litter biochar for bio-syngas production. Process Saf Environ Prot 109:478–488

Ren F, Li Z, Tan WZ, Liu XH, Sun ZF, Ren PG, Yan DX (2018) Facile preparation of 3D regenerated cellulose/graphene

oxide composite aerogel with high-efficiency adsorption towards methylene blue. J Colloid Interface Sci 532:58–67
Sehaqui H, Zhou Q, Berglund LA (2011) High-porosity aerogels of high specific surface area prepared from nanofibrillated cellulose (NFC). Compos Sci Technol 71(13):1593–1599
Silva FMF (2013) Estudo de materiais de isolamento térmico inovadores. Universidade do Porto, Porto
Skouteris G, Saroj D, Melidis P, Hai FI, Ouki S (2015) The effect of activated carbon addition on membrane bioreactor processes for wastewater treatment and reclamation—a critical review. Bioresour Technol 185:399–410
Wan C, Li J (2016) Graphene oxide/cellulose aerogels nanocomposite: preparation, pyrolysis, and application for electromagnetic interference shielding. Carbohydr Polym 150:172–179
Wiener M, Reichenauer G, Hemberger F, Ebert HP (2006) Thermal conductivity of carbon aerogels as a function of pyrolysis temperature. Int J Thermophys 27(6):1826–1843
Xiang C, Wang C, Guo R, Lan J, Lin S, Jiang S, Lai X, Zhang Y, Xiao H (2019) Synthesis of carboxymethyl cellulose-reduced graphene oxide aerogel for efficient removal of organic liquids and dyes. J Mater Sci 54(2):1872–1883
Xiao S, Gao R, Lu Y, Li J, Sun Q (2015) Fabrication and characterization of nanofibrillated cellulose and its aerogels from natural pine needles. Carbohydr Polym 119:202–209
Yang J, Zhang E, Li X, Zhang Y, Qu J, Yu ZZ (2016) Cellulose/graphene aerogel supported phase change composites with high thermal conductivity and good shape stability for thermal energy storage. Carbon 98:50–57
Zanini M, Lavoratti A, Zimmermann MVG, Galiotto D, Matana F, Baldasso C, Zattera AJ (2017) Aerogel preparation from short cellulose nanofiber of the Eucalyptus species. J Cell Plast 53(5):503–512
Zhang H, Fang WH, Li YM, Tao WQ (2017) Experimental study of the thermal conductivity of polyurethane foams. Appl Therm Eng 115:528–538
Zhao Y, Li Y, Zhang R (2018) Silica aerogels having high flexibility and hydrophobicity prepared by sol–gel method. Ceram Int 44(17):21262–21268
Zheng Q, Javadi A, Sabo R, Cai Z, Gong S (2013) Polyvinyl alcohol (PVA)-cellulose nanofibril (CNF)-multiwalled carbon nanotube (MWCNT) hybrid organic aerogels with superior mechanical properties. RSC Adv 3(43):20816–20823